Effect of Nonuniform Velocity Fields and Retrograde Flow on Distillation Tray Efficiency

The effect of nonuniform velocity distributions and retrograde flow on Murphree tray efficiency has been studied. Both types of nonuniformities were shown to substantially reduce the efficiency of the tray. The results show that the presence of flow nonuniformity alone may result in significant deviations from the efficiency predicted by the AIChE model.

RICHARD L. BELL
and
RODOLFO B. SOLARI

Department of Chemical Engineering
University of California
Davis, California 95616

SCOPE

Although tray-type contacting equipment has been in common use for years, the prediction of the mass transfer efficiency of these devices without data from similar services is at best imprecise. The most commonly used methods for predicting tray efficiency are based on that proposed in the AIChE Bubble Tray Design Manual (1958). This method first requires a prediction of gas and liquid phase transfer units which yield a point efficiency. The second step is to use the point efficiency in a mathematical model of liquid and gas motion on the tray to obtain an overall tray efficiency. These are separate steps and errors in either could independently result in errors in the prediction of tray efficiency.

The AIChE tray model assumes that the liquid phase flows from the tray inlet to outlet with a uniform velocity and with no velocity gradient in the direction normal to flow. However, it has recently been demonstrated that severe, nonuniform flow patterns exist on commercial-scale sieve trays (Bell, 1972a,b). These patterns ranged from simple nonuniform velocity distributions to extensive reverse or retrograde flow near the walls. In the latter case there was a high speed flow through the center of the tray and a tendency for pooling on either side of the centerline. The pooling resulted from regions in which the circulation was closed and as shown in the film by Keller and Yanagi (1970), the movement of fluid elements out of this region can be very slow. The AIChE Bubble Tray Design Manual, as well as other authors have drawn attention to the inefficiency which can accompany nonuniform flow distributions (Williams et al., 1960; Foss et al., 1958; Gerster et al., 1958). Although the effect of small-scale eddy dispersion on tray efficiency has been studied extensively, very little work has been done on the effects of deviation from the uniform velocity distribution.

Direct bypassing of fluid from the tray outlet to inlet was considered by Warzell (1955), Crozier (1955), and Oliver and Watson (1956). Strand (1963) experimentally determined a bypassing factor and showed that better agreement could be obtained between predicted and observed efficiencies by using his bypassing factor correlation. In each of these cases, however, a uniform velocity distribution was assumed and the bypassing stream did not participate in the mass transfer process.

Lebedev and co-workers (1968) have calculated the effect of a nonuniform velocity distribution by considering 2 flow paths which consist of several well mixed chambers. By use of this mixed hydrodynamic model the flow rate and mixing characteristics of each channel could be varied independently. They found that overall tray efficiency (EMV) could be substantially reduced depending on the combination of variables chosen in the model. More recently, Porter et al. (1972) has considered a model in which the fluid flows with uniform velocity through a channel of varying width in the center of the tray, flanked by stagnant pools. The two regions communicate by a mixing process. Concentration profiles similar to those reported by Bell (1972b) were obtained and again substantial reduction in efficiency was found depending on the parameters used.

The purpose of this study is to explore the effect on tray efficiency of nonuniform velocity distributions acting alone, without turbulent dispersion. Two variations will be considered. In the first a simple nonuniform velocity distribution across the tray without retrograde flow will we considered. In the second the effect of retrograde flow will be added to the nonuniform velocity distribution with mass transfer occurring in both the forward and retrograde flow paths.

CONCLUSIONS AND SIGNIFICANCE

This study has shown that the presence of nonuniform velocity distributions or retrograde flow alone can, in some cases, be expected to substantially reduce the efficiency of distillation trays. This effect is present in the absence of any turbulent mixing process. In severe cases the tray efficiency can be less than the point efficiency. The magnitude of the effect is strongly dependent on the magnitude of λEOG, the volume of liquid recycled in the retrograde stream and the fractions of the tray carrying the forward and retrograde streams.

These results indicate that efficiency data from trays on which nonuniform flow condition exist will probably not correlate well with efficiencies predicted by the AIChE method.

THEORETICAL MODEL

The coordinate system and the tray characteristics used in this model are shown in Figure 1. For computational simplicity a rectangular geometry has been used. The effect of a circular geometry in this model would be to increase the length of flow paths near the wall, thereby increasing the residence time of the respective fluid elements. This factor can be accounted for by changing the velocity distribution. Since the velocity distribution is to be a parameter, no generality will be sacrificed in the efficiency calculations using a rectangular geometry.

The Peclet numbers computed for the experiments in our previous work (Bell 1972a,b) have in general been in the range of 20 to 35 and are sufficiently high that little error is introduced by setting them equal to infinity. The Peclet numbers were obtained from the correlations recommended in the AIChE Bubble Tray Design Manual (1958) and are for the component of mixing in the direction of flow. In the presence of a nonuniform velocity field, concentration gradients normal to the direction of flow are established and the mixing component across these gradients could be significant. However, in this model we take the limiting case in which the Peclet number in all directions is infinite in order to isolate the effects of nonuniform flow. It is further assumed that there are no concentration gradients in the liquid phase in the direction normal to the tray. If the usual assumption of linear equilibrium is made, the general point equation of change takes the form shown in Equation (1).

$$\mathbf{q} \cdot \nabla x_n - \lambda EOG\,(x^*_{n+1} - x_n) = 0 \qquad (1)$$

The vector $\mathbf{q}$ is defined in Equation (2) and represents the velocity field normalized by the average velocity $\bar{v}$ which would exist in a uniform flow field with the same geometry and average flow rate.

$$\mathbf{q}\bar{v} = \mathbf{v} \qquad (2)$$

Solutions were now sought for Equation (1) in which $\mathbf{q}$ is an arbitrary velocity distribution which may include retrograde flow. λEOG is taken to be constant but not necessarily the same in the forward and retrograde flow path, and the inlet vapor to the tray is of uniform composition. The two cases of simple nonuniform flow and nonuniform retrograde flow will be considered separately.

SIMPLE NONUNIFORM FLOW

Simple nonuniform flow is characterized by the presence of a velocity distribution but no retrograde flow. If the velocity field is taken as rectilinear, the $\mathbf{q}$ vector has only one nonzero component and depends only on the coordinate normal to the flow. For this case Equation (1) can be written

$$\frac{dx_n(Z,\xi)}{dZ} - \frac{\lambda EOG}{q(\xi)}\left[x^*_{n+1} - x_n(Z,\xi)\right] = 0 \qquad (3)$$

Integration with the boundary condition that the concentration of the liquid entering the tray x_{n0} is uniform yields the concentration profile at any position ξ.

$$\frac{x^*_{n+1} - x_n(Z,\xi)}{x^*_{n+1} - x_{n0}} = \exp\left[-\lambda\frac{EOG}{q(\xi)}Z\right] \qquad (4)$$

This is similar to the Lewis Case I result (Lewis, 1936) except for the velocity distribution in the denominator of the exponential argument.

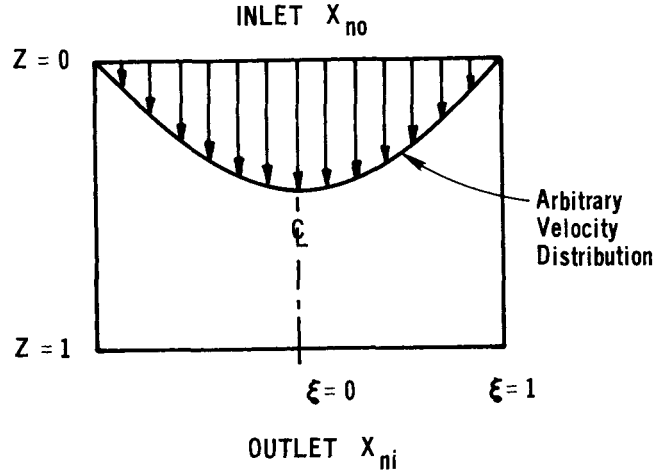

Fig. 1. Schematic diagram of a simple nonuniform flow distribution.

The definition of the overall Murphree tray efficiency is

$$EMV = \frac{\bar{y}_n - y_{n+1}}{y^*_{n1} - y_{n+1}} \qquad (5)$$

where $\bar{y}_n$ is the average vapor composition from the tray, $\overline{y^*_{n1}}$ is the vapor in equilibrium with the average liquid leaving the tray, and y_{n+1} the vapor composition entering the tray. Equation (4) can be used to compute the average liquid composition leaving the tray by setting Z equal to unity and integrating $x(1,\xi)$ over ξ weighted by $q(\xi)$. Again using the assumption of linear equilibria, the following expression for the vapor in equilibrium with the average liquid leaving the tray is obtained:

$$\frac{\overline{y^*_{n1}} - y_{n+1}}{m(x_{n0} - x^*_{n+1})} = \int_0^1 q(\xi)\exp\left[-\frac{\lambda EOG}{q(\xi)}\right]d\xi \qquad (6)$$

It should be noted that the integral of $q(\xi)$ from 0 to 1 is unity and consequently does not appear as a normalizing factor in Equation (6).

To compute the average composition of the vapor leaving the tray it is convenient to use the definition of point efficiency shown in Equation (7).

$$EOG = \frac{y_n(Z,\xi) - y_{n+1}}{y^*_n - y_{n+1}} \qquad (7)$$

Using the equilibrium expression to convert the denominator of Equation (7) into liquid phase mole fraction and substituting into Equation (4) yields Equation (8)

$$\frac{y_n(Z,\xi) - y_{n+1}}{m\,EOG(x_{n0} - x^*_{n+1})} = \exp\left[-\frac{\lambda EOG}{q(\xi)}Z\right] \qquad (8)$$

To get the average vapor composition $\bar{y}_n(\xi)$ along any flowpath ξ Equation (8) is integrated with respect to Z. Since the vapor flow rate is considered to be uniform across the tray no vapor flow weighting factor is required and the resultant expression is

$$\frac{\overline{y_n(\xi)} - y_{n+1}}{m(x_{n0} - x^*_{n+1})} = \frac{q(\xi)}{\lambda}\left[1 - \exp\left(-\frac{\lambda EOG}{q(\xi)}\right)\right] \qquad (9)$$

To get the average vapor composition for the entire tray $\bar{\bar{y}}_n$, Equation (9) is now integrated with respect to ξ to yield

$$\frac{\bar{\bar{y}}_n - y_{n+1}}{m(x_{no} - x^*_{n+1})} = \int_0^1 \frac{q(\xi)}{\lambda}\left[1 - \exp\left(-\frac{\lambda EOG}{q(\xi)}\right)\right] d\xi \quad (10)$$

From the definition of the overall Murphree tray efficiency in Equation (5) the ratio EMV/EOG for the case of simple nonuniform flow can be expressed as the ratio of integrals from Equations (10) and (6).

$$\frac{EMV}{EOG} = \frac{\int_0^1 \frac{q(\xi)}{\lambda EOG}\left[1 - \exp\left(\frac{\lambda EOG}{q(\xi)}\right)\right] d\xi}{\int_0^1 q(\xi) \exp\left(-\frac{\lambda EOG}{q(\xi)}\right) d\xi} \quad (11)$$

Equation (11) was integrated numerically using the three velocity distributions shown in Figure 2. The velocity distributions were assumed to be symmetric around the tray centerline. The solutions were found to be convergent for $\Delta\xi = 0.005$ (200 parallel paths) for the results in this section and the nonuniform retrograde flow theory in the following section.

Three velocity distributions were studied which represented severe to moderate intensities of flow nonuniformity. The inverted parabolic distribution is characteristic of severe channeling along the centerline and is the most intense nonuniformity. The parabolic distribution more closely approaches uniform flow and consequently is the least intense nonuniformity. In each case the distributions are normalized to a mean velocity of unity and incorporate slip at the wall in terms of the parameter q_s which is a fraction of the mean velocity. The equations for the velocity distributions are

Case I Inverted parabolic

$$q(\xi) = 3(1 - q_s)(1 - \xi)^2 + q_s \quad (12)$$

Case II Linear $q(\xi) = 2(1 - q_s)(1 - \xi) + q_s \quad (13)$

Case III Parabolic $q(\xi) = \frac{3}{2}(1 - q_s)(1 - \xi^2) + q_s \quad (14)$

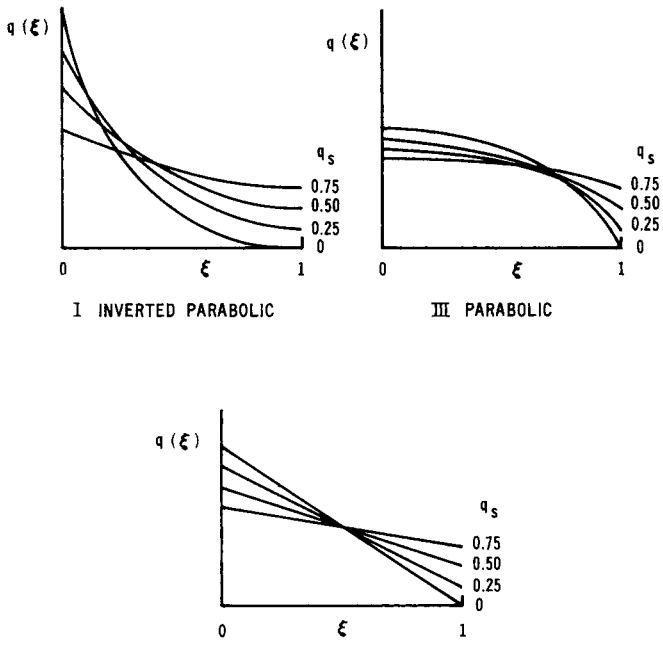

Fig. 2. The velocity distributions used in the calculation of efficiency using the simple nonuniform flow model.

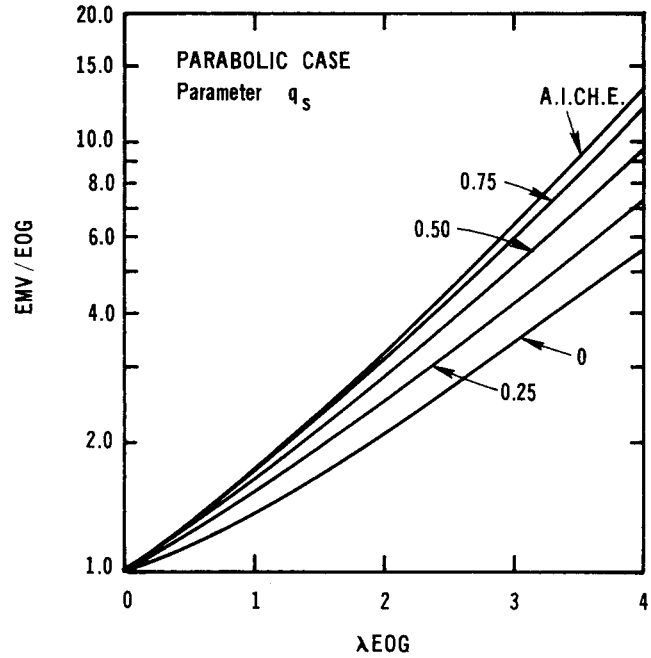

Fig. 3. The effect of a parabolic velocity distribution on tray efficiency with wall slip as a parameter.

RESULTS FROM THE SIMPLE NONUNIFORM FLOW MODEL

The results for the parabolic and inverted parabolic velocity distributions are compared to the AIChE case for infinite Peclet number in Figures 3 and 4, respectively. The intensity of the flow nonuniformity as characterized by the slip velocity q_s is similar in effect to the Peclet number in the AIChE model. As the intensity of the nonuniformity increases the overall tray efficiency is substantially reduced with maximum reduction occurring at high values of λEOG. A significant feature is that for severe channeling, such as present in the inverted parabolic case, the EMV/EOG ratio can become less than unity.

A comparison of the relative effect of the intensity of flow nonuniformity as characterized by the shape of the velocity distribution is shown in Figure 5 for the no wall slip ($q_s = 0$) cases. The linear case is intermediate in intensity of flow nonuniformity and consequently is intermediate in effect. In every case the presence of a simple nonuniform flow with no turbulent dispersion, causes a substantial reduction in efficiency from that predicted for uniform flow.

NONUNIFORM RETROGRADE FLOW

The basic model for nonuniform retrograde flow is shown schematically in Figure 6. This model is distinguished from the simple nonuniform flow model by the presence of retrograde flow paths on either side of the forward flow path. The two regions are separated by a line along which the velocity must be zero. The forward flow path occupies a fraction β of the total tray area, and consequently for a rectangular tray the line of zero flow must be located a distance β from the centerline on normalized half plane coordinates. At the outlet a volume of liquid corresponding to a fraction α of the liquid coming to the tray is diverted into the retrograde flow paths near the walls. Visual observation of the flow pattern on sieve trays has shown a significant component of flow parallel to the outlet weir with the fluid rotating around lines which are symmetric and parallel to the centerline (Keller and Yanagi, 1970). In some cases the

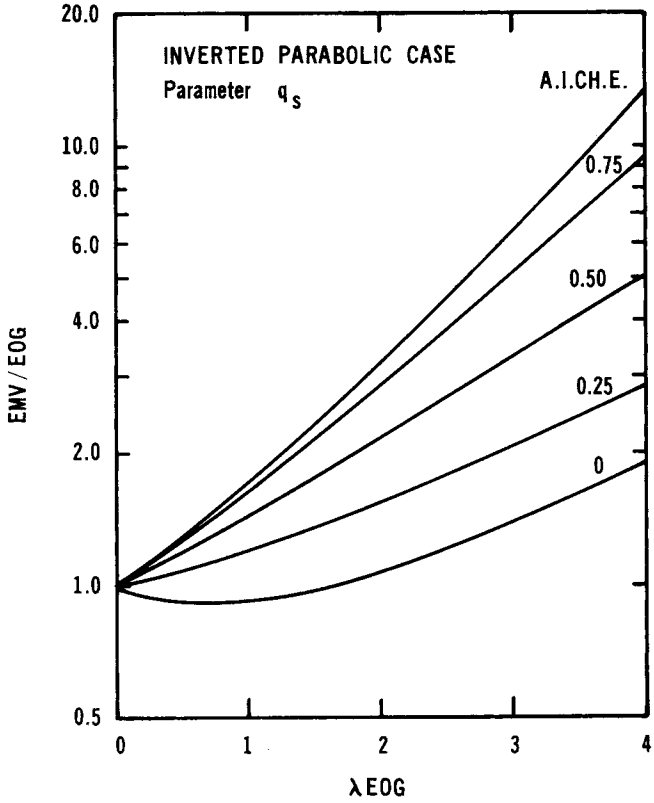

Fig. 4. The effect of an inverted parabolic velocity distribution on tray efficiency with wall slip as a parameter.

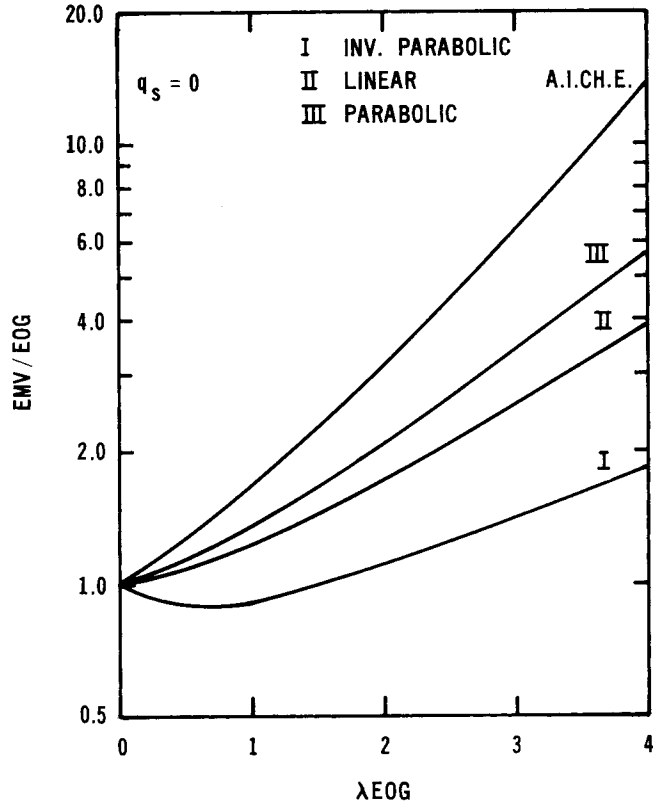

Fig. 5. Comparative effect of the shape of the velocity distribution on tray efficiency.

retrograde stream penetrates into the downcomer, in others it flows parallel to the inlet apron and becomes rapidly mixed with incoming fluid in the region of the hydraulic jump at the tray inlet. Based on these observations and residence time data from the bottom of downcomers (Bell, 1972b) the retrograde stream was assumed to mix thoroughly with the incoming liquid before the liquid reaches the tray. At the tray outlet three models were considered which dealt with the details of how the fluid is diverted at the weir.

In the first model, shown schematically in Figure 7, it is assumed that the fluid from the forward flow path is completely mixed at the outlet and then an appropriate amount is introduced into the retrograde channel. Since in this case the fluid entering the retrograde path has uniform composition, this model will be referred to as the uniform composition model. In the second model the flow paths are rotated off the tray, as shown in Figure 8, so that the fluid from a flow line near the center of the tray rotates to a position near the wall. In this case the fluid composition varies across the inlet to the retrograde path. We will refer to this model as the external rotation model. A variation of this model was also considered, in which fluid rotation was started inside the trap at a distance $Z = \beta$ from the inlet. The two rotational models gave results so nearly identical that only the external rotation model will be discussed in detail.

If the total volumetric flow rate to the tray is Q and the volume of fluid being recycled along the retrograde path is αQ, then the inlet fluid composition is given by Equation (15).

$$x_{n0} = \frac{x_{n-1} + \alpha x_{m0}}{1 + \alpha} \qquad (15)$$

The term x_{m0} is the mixing cup average composition of the fluid leaving the retrograde path.

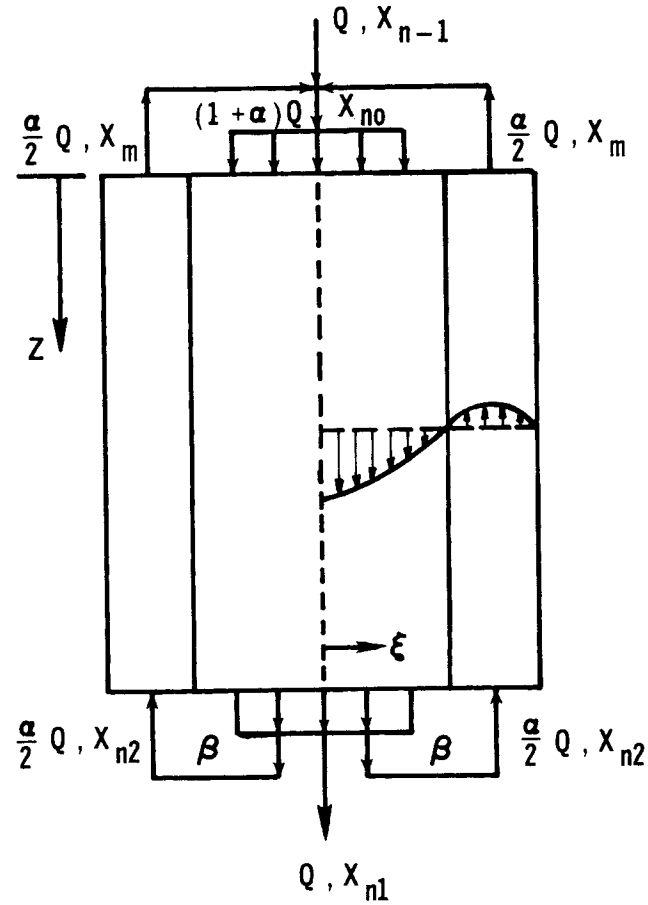

Fig. 6. Schema for the nonuniform retrograde flow model.

By methods similar to those employed in the previous section for the simple nonuniform velocity distribution case, the following equations can be derived for the retrograde cases:

Uniform Composition Model

$$\frac{EMV}{EOG} = \frac{1}{\lambda EOG}\left[\frac{1}{\gamma_1 k_1}\int_0^{\beta} q(\xi)\left[1-\exp\left(-\frac{A}{q(\xi)}\right)\right]d\xi - \frac{1}{\gamma_2}\int_{\beta}^{1} q(\xi)\left[1-\exp\left(\frac{B}{q(\xi)}\right)\right]d\xi\right] \quad (16)$$

where k_1, A, B, γ_1, and γ_2 are defined as follows:

$$k_1 = \frac{1}{1+\alpha}\int_0^{\beta} q(\xi)\exp\left(-\frac{A}{q(\xi)}\right)d\xi \quad (17)$$

$$\gamma_1 = \frac{\beta}{1+\alpha} \quad (18)$$

$$\gamma_2 = \frac{1-\beta}{\alpha} \quad (19)$$

$$A = \gamma_1 \lambda EOG \quad (20)$$

$$B = \gamma_2 \lambda EOG \quad (21)$$

External Rotation Model

$$\frac{EMV}{EOG} = \frac{1}{\lambda EOG}\left[\frac{\frac{1}{\gamma_1}\int_0^{\beta} q(\xi)\left[1-\exp\left(-\frac{A}{q(\xi)}\right)\right]d\xi + \frac{1}{\gamma_2}\int_{\beta}^{1} q(\xi)E(\xi)\left[\exp\left(\frac{B}{q(\xi)}\right)-1\right]d\xi}{\int_0^{\xi_0} q(\xi)\exp\left(-\frac{A}{q(\xi)}\right)d\xi}\right] \quad (22)$$

where $E(\xi)$ is given by Equation (23)

$$E(\xi) = \exp\left(-\frac{A}{q((1+\delta)\beta - \delta\xi)}\right) \quad (23)$$

and ξ_0 is calculated by solving Equation (24)

$$\int_{\xi_0}^{\beta} q(\xi)d\xi = \alpha \quad (24)$$

The scale factor δ, as given by Equation (26), represents the ratio of the forward flow area involved in recirculation to the retrograde flow area. This factor arises in the boundary condition representing the flow rotation at the weir as shown in Equation (25).

$$x_{n2}(\xi) = x_{n1}((1+\delta)\beta - \delta\xi) \quad \xi > \beta \quad (25)$$

$$\delta = (\beta - \xi_0)/(1-\beta) \quad (26)$$

Again in this analysis the velocity profile $q(\xi)$ can be specified and the integrations carried out numerically. In this case, however, conservation relationships impose the following restrictions on $q(\xi)$:

$$\int_0^{\beta} q(\xi)d\xi = 1+\alpha \quad (27)$$

$$\int_{\beta}^{1} q(\xi)d\xi = \alpha \quad (28)$$

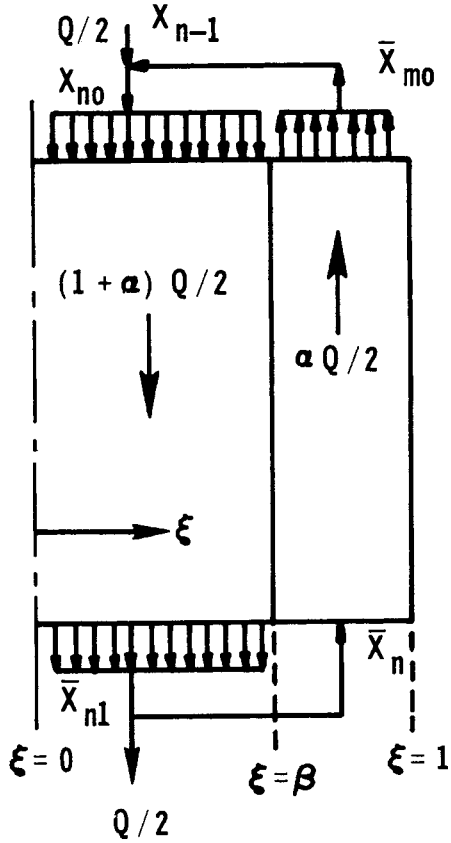

Fig. 7. Schematic diagram of the uniform composition, retrograde flow model.

The velocity distributions used for the retrograde case are shown in Equations (29) to (34). It should be noted that on the line of rotation at $\xi = \beta$ the velocity must be zero.

Case I Inverted Parabolic

$$q(\xi) = 3\frac{(1+\alpha)}{\beta^3}(\xi-\beta)^2 \quad \xi < \beta \quad (29)$$

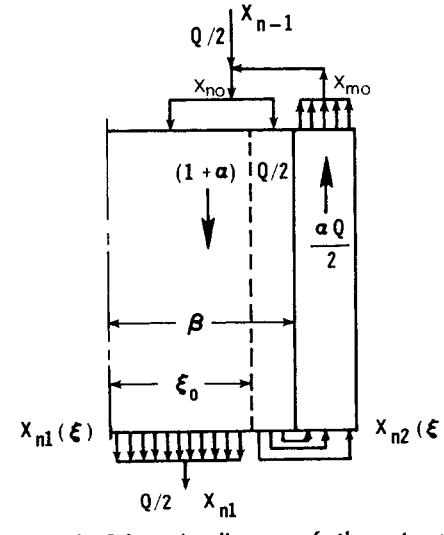

Fig. 8. Schematic diagram of the external rotation, retrograde flow model.

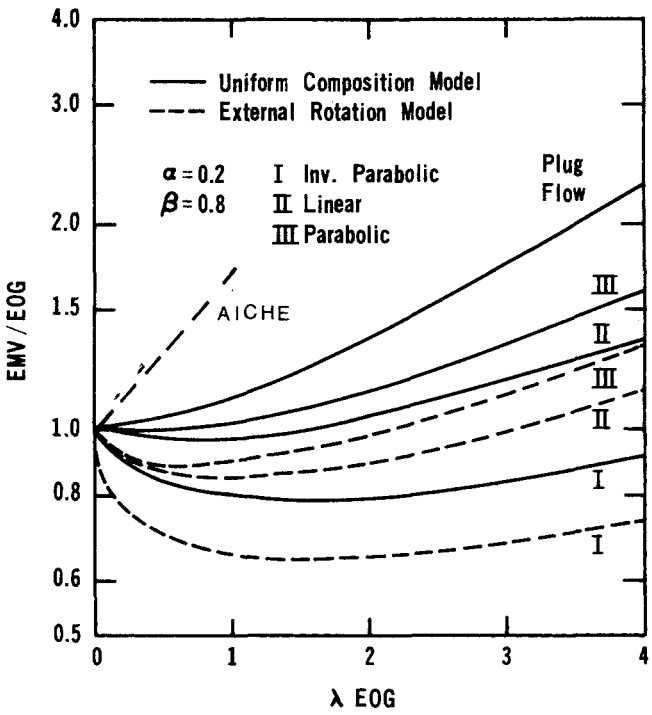

Fig. 9. Comparison of the effect on tray efficiency of the uniform composition and external rotation, retrograde flow assumptions for $\beta = 0.8$ and $\alpha = 0.2$.

$$q(\xi) = \frac{3\alpha}{(1-\beta)^3}(\xi - \beta)^2 \quad \xi > \beta \tag{30}$$

Case II Linear

$$q(\xi) = \frac{2(1+\alpha)}{\beta^2}(\beta - \xi) \quad \xi < \beta \tag{31}$$

$$q(\xi) = \frac{2\alpha}{(1-\beta)^2}(\beta - \xi) \quad \xi > \beta \tag{32}$$

Case III Parabolic

$$q(\xi) = \frac{3(1+\alpha)}{2\beta^3}(\beta^2 - \xi^2) \quad \xi < \beta \tag{33}$$

$$q(\xi) = \frac{3\alpha}{2(1-\beta)^3}(\beta^2 - \xi^2) \quad \xi > \beta \tag{34}$$

RESULTS FROM THE NONUNIFORM RETROGRADE FLOW MODEL

The combined effect of velocity nonuniformities and retrograde flow on overall tray efficiency is shown in Figures 9 and 10. For the sake of brevity, only two cases are presented here. Other combinations of the parameters α and β yield curves with similar characteristics. It is clear from Figures 9 and 10 that tray efficiency is substantially affected by retrograde flow even if uniform velocity distribution (plug flow) is assumed for each path. The effect of the retrograde stream mixing with the rich liquid entering the tray is to reduce the concentration driving force for mass transfer. Tray efficiency increases with increasing β as shown in Figure 11 due to the fact that more of the tray area is used for contacting vapor with incoming liquid and the tray more closely approximates the ideal case.

The influence of the recirculation parameter α on tray efficiency is also shown in Figure 11. When recirculation takes place on a large fraction of the tray (β small), most of the fresh liquid flows through a narrow central region causing channeling and bypassing and the tendency is for values of EMV/EOG less than unity. In this case increasing α increases the efficiency of the tray by driving it toward the perfectly mixed case ($EMV/EOG = 1$). If β is large, increasing α again drives the tray toward the perfectly mixed situation but in this case the efficiency of the tray is reduced.

Figures 9 and 10 show that the uniform composition model always yields higher tray efficiency than the rotational model. In the rotational model it is only those fluid elements with long residence time and consequently low concentration which are recycled. The driving force for mass transfer in the retrograde circulation area will therefore be higher for the uniform composition model than for the recirculation model. It should be emphasized that

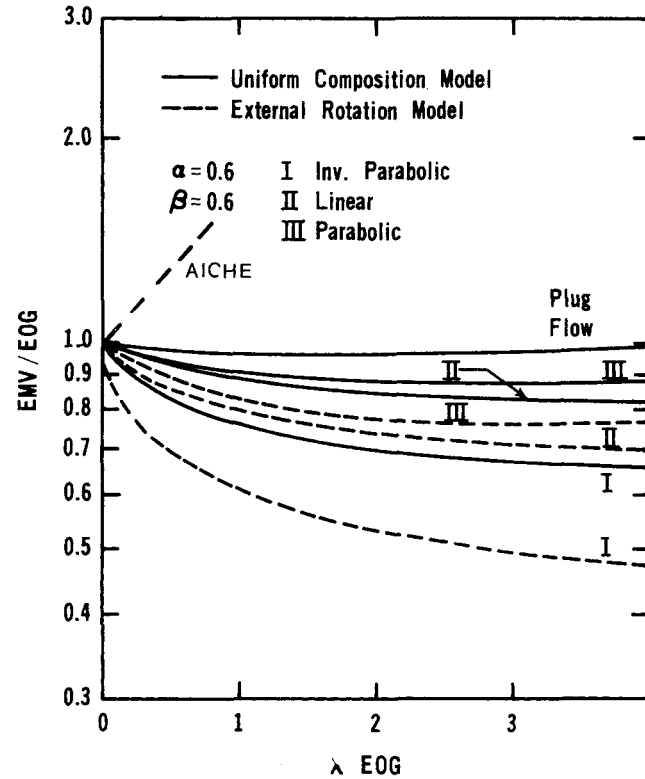

Fig. 10. Comparison of the effect on tray efficiency of the uniform composition and external rotation, retrograde flow assumptions for $\beta = 0.6$, $\alpha = 0.6$.

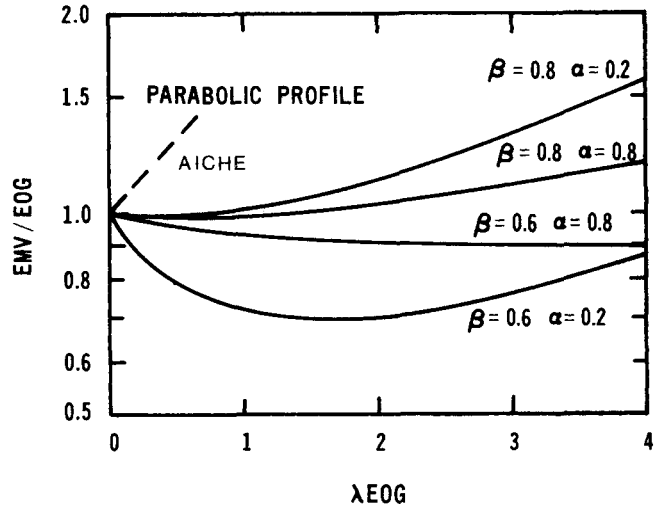

Fig. 11. The effect of the parameters α and β on tray efficiency.

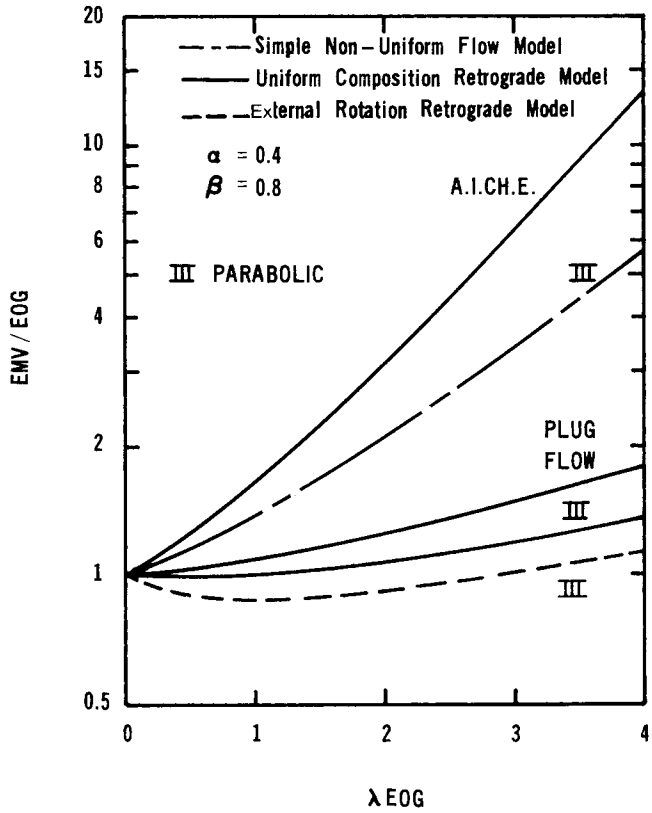

Fig. 12. The relative effect of the three types of flow nonuniformity for a parabolic velocity distribution and a comparison to the AIChE model and retrograde plug flow.

the rotational model is closer to the actual performance of large size trays than the uniform composition model. From observation of tray behavior (Keller and Yanagi, 1970) it appears unlikely that the assumption of perfect mixing at the weir is met in practical situations.

DISCUSSION

The results of this study clearly indicate that even though the Peclet number is high, the presence of nonuniform or retrograde flow patterns can affect the Murphree tray efficiency rather substantially. The magnitude of the effect depends as before on λEOG, but in this case the parameter is the velocity distribution rather than the Peclet number. In Figure 12 the relative effects of the velocity distribution are summarized.

A simple parabolic velocity distribution with no slip at the wall has the same effect as a Peclet number of about 8 in the AIChE model. The effect of adding a retrograde flow path is to reduce the efficiency even further. Assuming plug flow in the forward and retrograde paths and uniform composition model is equivalent to a Peclet number of about 1.5, for $\beta = 0.8$ and $\alpha = 0.4$. If parabolic flow in the forward and retrograde paths is assumed the result is equivalent to a Peclet number of about 0.5 for the uniform composition model. Since the ratio EMV/EOG is less than unity for the rotation model, there is no corresponding case in the AIChE analysis.

By proper selection of α, β, and the velocity distribution virtually any desired effect can be obtained. At this juncture very little is known about the detailed flow structure on trays. Consequently precise values of α and β are not available nor can a specific flow distribution be assigned to a specific tray.

A recent report by Yanagi and Scott (1973) shows that there was virtually no difference in efficiency between trays on which retrograde flow was known to exist and trays in exactly the same service on which the flow had been straightened. The systems used in the study had values of λEOG on the order of unity. Except for the severe cases of channeling ($EMV/EOG < 1.0$), the effects of flow nonuniformity are somewhat less in this range than at higher values of λEOG. However, the nearly perfect agreement between the efficiency results would indicate that whatever the flow conditions they were such that they did not substantially effect efficiency. This suggests that for the tray geometries used in their study the value of β must be high and the value of α low. Verification of this conclusion must await more detailed studies of the flow patterns on real trays.

ACKNOWLEDGMENT

R. B. Solari gratefully acknowledges the financial support of the Ford Foundation through the University of Chile-University of California Cooperative Program. This work was supported by grant number NSF GK 30370 from the National Science Foundation.

NOTATION

A = defined by Equation (20)
B = defined by Equation (21)
EOG = Murphree point efficiency
EMV = overall Murphree tray efficiency
$E(\xi)$ = defined by Equation (23)
k_1 = defined by Equation (17)
m = slope of the vapor-liquid equilibrium curve
P_e = Peclet number
$q(\xi)$ = normalized velocity profile function
q_s = slip velocity at the wall
Q = total volumetric flow rate into the tray
$x_n(Z, \xi)$ = liquid composition at any point on the tray
x_{n-1} = inlet liquid composition
$x_{n1}(\xi)$ = outlet liquid composition
$x_{n2}(\xi)$ = liquid composition at the inlet of the retroflow zone
x_{m0} = mixing cup average composition of the fluid leaving the retrograde paths
x_{n0} = liquid composition at the inlet of the tray
x^*_{n+1} = liquid composition in equilibrium with the inlet vapor
x_n = liquid composition at any point in space
$y_n(Z, \xi)$ = vapor composition at any point on the tray
y_{n+1} = inlet vapor composition
$\overline{y_n}(\xi)$ = average vapor composition along any ξ path
$\overline{\overline{y_n}}$ = outlet average vapor composition
y^*_n = vapor composition in equilibrium with liquid composition x_n
$\overline{y^*_{n1}}$ = vapor composition in equilibrium with the average liquid leaving the tray
$\mathbf{v}$ = liquid velocity
$\bar{v}$ = average liquid velocity
Z = ordinate in the liquid flow direction

Greek Letters

α = fraction of the liquid recycled
β = central area/total area of the tray
γ_1 = defined by Equation (18)
γ_2 = defined by Equation (19)
λ = stripping factor on the total tray
ξ = ordinate in the direction normal to the flow
ξ_0 = defined in Figure 8, Equation (24)
δ = scale factor defined by Equation (26)

Note: All the compositions are in the molar fraction.

LITERATURE CITED

AIChE, "Bubble Tray Design Manual, Prediction of Fractionation Efficiency," *AIChE*, New York (1958).

Bell, R. L., "Experimental Determination of Residence Time Distributions on Commercial Scale Distillation Trays using a Fiber Optic Technique," *AIChE J.*, **18**, 491 (1972a).

———., "Residence Time and Fluid Mixing on Commercial Scale Sieve Trays," *ibid.*, **18**, 498 (1972b).

Crozier, R. S., Ph.D. thesis, Univ. of Michigan, Ann Arbor (1955).

Foss, A. S., J. A. Gerster, R. L. Pigford, "Effect of Liquid Mixing on the Performance of Bubble Trays," *AIChE J.*, **4**, 231 (1958).

Gerster, J. A., A. B. Hill, N. N. Hochgraf, D. B. Robinson, "Tray Efficiencies in Distillation Columns," Final Report, Univ. of Delaware, Newark (1958).

Keller, G. J., and T. Yanagi, Film, "Fluid Flow on Fractionation Trays," paper presented at AIChE 68th National Meeting (1970).

Lebedev, Y. N., I. A. Aleksandrov, and D. D. Zykov, "Combined Hydrodynamic Models of Fractionating Column Trays under Crossflow Conditions," *Teor. Osnovy Khim. Tekhno.*, **2**, 2, 183 (1968).

Lewis, W. K., "Rectification of Binary Mixtures. Plate Efficiency of Bubble Cap Columns," *Ind. Eng. Chem.*, **28**, 399 (1936).

Oliver, E. D. and C. C. Watson, "Correlation of Bubble-Cap Fractionating-Column Plate Efficiencies," *AIChE J.*, **2**, 18 (1956).

Porter, K. E., M. J. Lockett, and C. T. Lim, "The Effect of Liquid Channeling on Distillation Plate Efficiency," *Trans. Instn. Chem. Engrs.*, **50**, 91 (1972).

Strand, C. P., "A New Look at Distillation.—Bubble Cap Tray Efficiencies," *Chem. Eng. Progr.*, **59**, 58 (1963).

Warzell, L., Ph.D. thesis, Univ. of Michigan, Ann Arbor (1955).

Williams, B., J. W. Begley, and C. Wu, "Tray Efficiencies in Distillation Columns." AIChE Research Committee, Univ. of Michigan Final Report (1960).

Yanagi, T., and B. D. Scott, "Effect of Liquid Mixing on Sieve Trays," *Chem. Eng. Progr.*, **69**, 75 (1973).

Manuscript received August 18, 1972; revision received March 12 and accepted March 13, 1974.

Statistical Characteristics of Thin, Wavy Films:

Part II. Studies of the Substrate and its Wave Structure

Waves on falling liquid films display certain random features. At least two classes of such random waves are shown to exist; large waves which carry the bulk of the fluid and small waves which cover a substrate film that exists between large waves. It is shown that the statistics of the substrate thickness and its wave structure can be extracted from measurements of the variation of film thickness with time. A theory is presented for calculating the mean substrate thickness and the substrate flow rate. The statistics of the wave structure is presented and compared with existing theory. The importance of the substrate in controlling transfer processes is demonstrated.

K. J. CHU
and
A. E. DUKLER

Chemical Engineering Department
University of Houston
Houston, Texas 77004

SCOPE

The flow of thin liquid films occurs in a wide variety of process equipment including falling film evaporators, reactors and wetted wall towers, thermosyphon reboilers, direct fired tubular boilers, and pipeline reactors. Experimental observations have shown that in almost all cases of practical interest the liquid displays random waves at the interface and that rates of transfer of heat and mass are greatly enhanced by the presence of these waves (Dukler, 1972). The use of simple transport equations and the assumption of a smooth interface fail to describe the process accurately and, as a result, the reliability of design procedures for such process equipment has been inadequate (Alves, 1970). Improving design procedures for thin, wavy film systems requires information on the wave structure and the manner in which the waves change the velocity fields in the liquid and gas phases bounded by the interface. But the wave structure has been shown to be a complex one. There appear to be several classes of waves and each class has certain random features. In particular, it is already known (Telles and Dukler, 1970) that the interface consists of waves large in amplitude compared to the film thickness which are separated by a very thin liquid substrate, itself covered by small waves. The substrate plays an important role in determining transport of heat and mass through the film. The purpose of this paper is to present new methods for extracting the meaningful statistical information about the substrate and its wave structure and to interpret the results of a very detailed study of that substrate under a variety of conditions of flow and shear. This hydrodynamic data can then provide the information needed to model the transfer processes. A subsequent paper in the series will discuss the large wave structure.

CONCLUSIONS AND SIGNIFICANCE

New data on the statistics of the substrate and its associated wave structure are presented for a wide range of liquid and gas rates covering flow situations of importance in film flow type process equipment. A method of time series analyses is presented which permits the statistics of the substrate to be extracted from the statis-

Correspondence concerning this paper should be addressed to A. E. Dukler.